

## Supplementary information

*for*

### **Emerging investigator series: Suspended air nanobubbles in water can shuttle polystyrene nanoplastics to air-water interface**

Kenneth Mensah<sup>a</sup>, Sudheera Yaparathne<sup>a</sup>, Andre L. Magdaleno<sup>b</sup>, Sergi Garcia-Segura<sup>b</sup>, Onur G.

Apul<sup>\*a</sup>

<sup>a</sup> Department of Civil and Environmental Engineering, University of Maine, Orono, ME 04469,  
United States

<sup>b</sup> School of Sustainable Engineering and the Built Environment, Arizona State University,  
Tempe, AZ 85287, United States

**\*Corresponding author:** email: [onur.apul@maine.edu](mailto:onur.apul@maine.edu); Phone: +1 207.581.2981 Fax:  
207.581.3888

## **Text S1**

### **Materials and reagents**

100 nm polystyrene (PS) latex indicator standard (0.01% weight/volume) was purchased from Malvern Panalytical and used as a model nanoplastic. PS is the most utilized plastic polymer for plastic pollution and toxicity studies.<sup>1-35</sup> Sodium hydroxide (analytical grade, 99%) and hydrochloric acid (ACS reagent grade, 37%) were procured from Acros Organics.

### **Nanobubble generation**

Air nanobubbles were generated in a 32-gallon nanopure water (NW) using a Moleaer XTB 25 generator. The system was made up of a gas pressure of 100 PSIG, a gas flow rate of 1 LPM, and 13 PSI water pumping pressure for 1 h. The generated nanobubbles were transferred to 1 L polypropylene bottles, ensuring it was filled to the brim with no headspace, and then stored in a refrigerator at 4 °C. The number concentration and size distribution of the bubble were analyzed using NanoSight NS 300.

## Text S2

### UV-vis spectroscopy

The concentration of nanoplastics was analyzed using a Hach DR 6000 UV-vis spectrophotometer in a 1 cm plastic cuvette at a wavelength of 249 nm. To ensure data reliability in the measurements, each experiment was performed in triplicates and each sample was measured at least five times with the UV-vis spectrophotometer, and the average of three close values was selected. The concentrations of nanoplastics were determined using a linear equation generated from the calibration curve (Fig. S1) that relates the absorbance to concentration. The calibration curve in Fig. S1 shows that nanoplastics can be detected in both DI water and nanobubble solution without any interference by the nanobubbles.

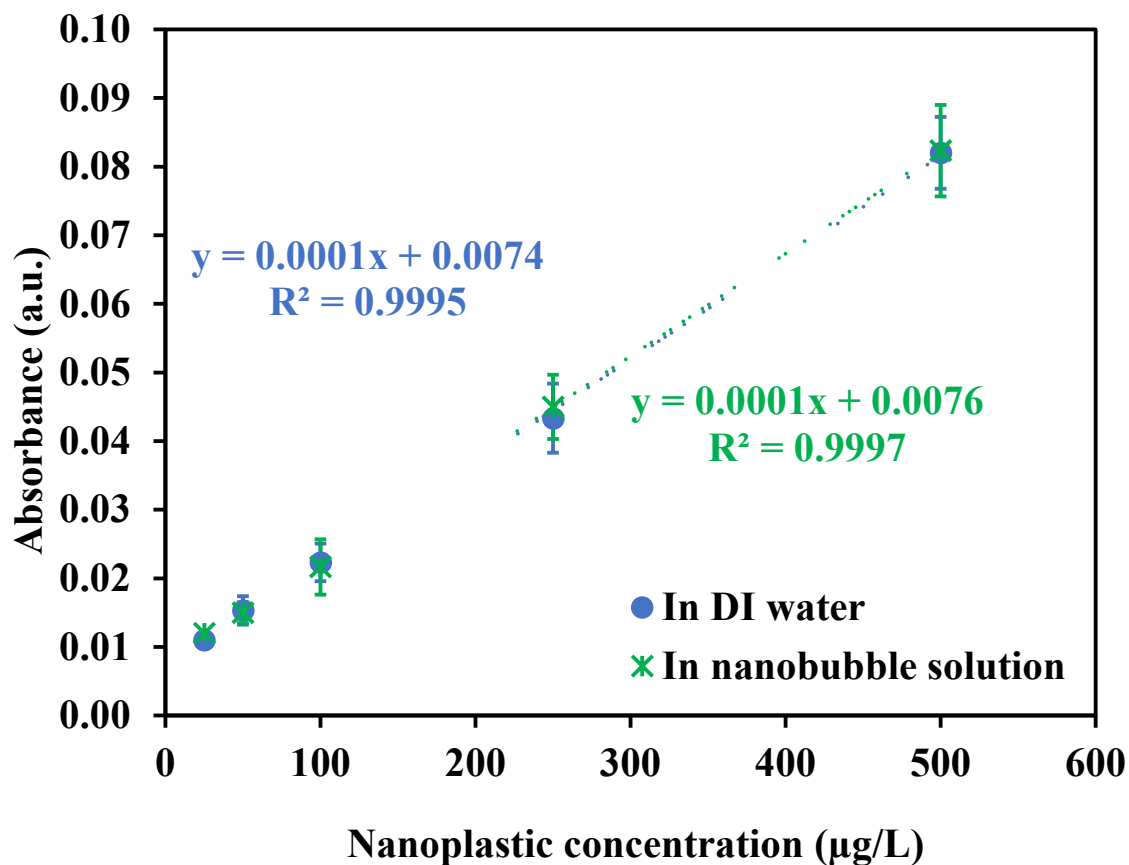


Fig. S1. UV-vis calibration curve for nanoplastics in nanopure and nanobubble water.

## Nanoparticle Tracking Analysis (NTA)

NanoSight NS300 (Malvern Panalytical, UK) was employed for the assessment of number concentration, average size, and size distribution of triplicate 1 mL samples of nanoplastics, nanobubbles, and the mixture of nanoplastics and nanobubbles. The instrument characterizes nano-entities (particles and bubbles) based on the nanoparticle tracking analysis (NTA) principle as explained elsewhere.<sup>36,37</sup> Our NanoSight NS300 is equipped with a green laser and a syringe pump. Each measurement entailed 60 seconds of video recording at a camera level of 13-15. The detection threshold was set at 5-20. The NTA software analyzed five consecutive video recordings for each NanoSight measurement, producing a number/size distribution, with the reported results representing the averages and standard error.

## Zeta potential

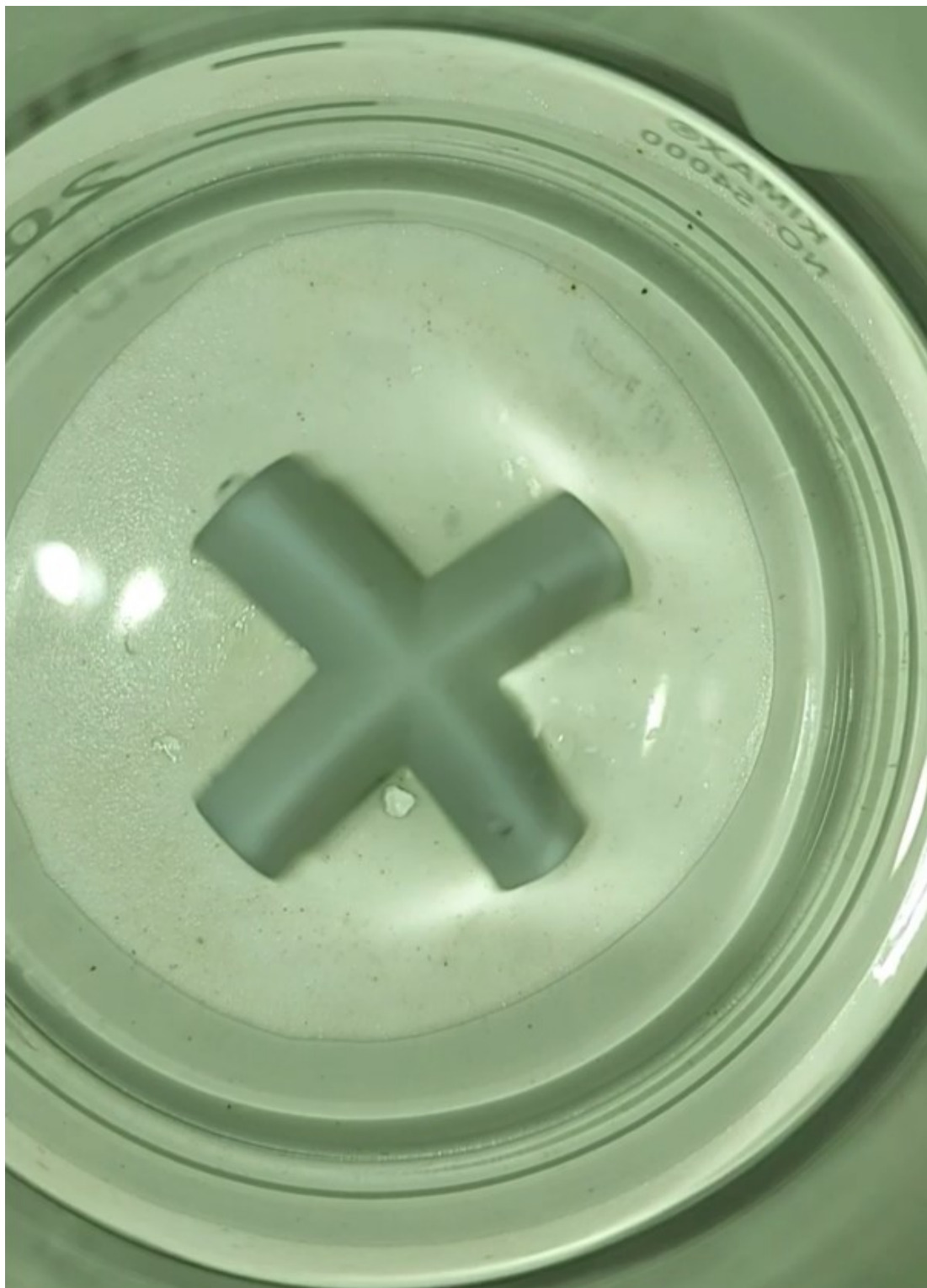
The zeta potential of the nanobubbles and nanoplastics from triplicate measurements was analyzed using Zetasizer Nano-ZS. For each sample, the initial and final pH after the experiment, presented in Table S1 with the standard error (SE), was measured using MultiLab IDS 4010-3W. Prior to the zeta potential measurement, the refractive index and absorption values of nanobubbles and nanoplastics were set as shown in Table S2. The dispersant was set to water with temperature = 25 °C, viscosity = 0.8872 cP, refractive index = 1.330, and dielectric constant = 78.5. Samples were loaded in a DTS1060C-Clear zeta cell and the equilibration time was set to 120 s. The zeta potential was automatically calculated by the Zetasizer Nano-ZS software using the Smoluchowski model and an F(Ka) value of 1.5. As a control measurement, the zeta potential of DI water was measured to be  $-0.75 \pm 0.37$ .

**Table S1** Changes in pH before and after stirring

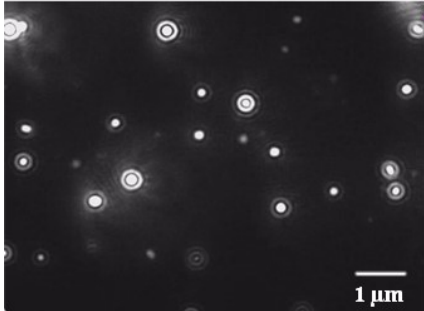
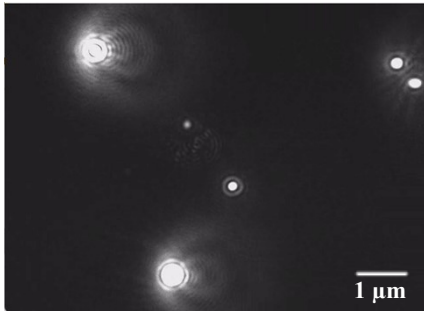
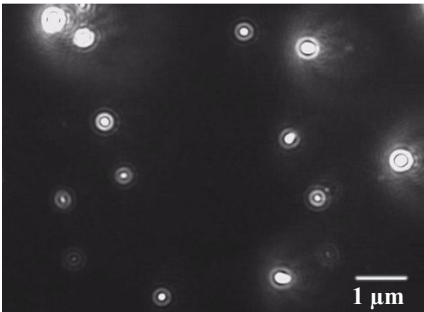
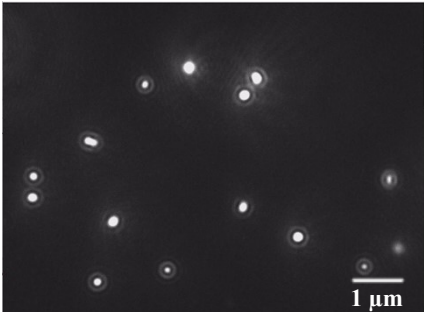
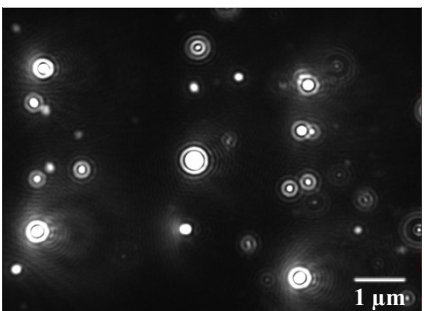
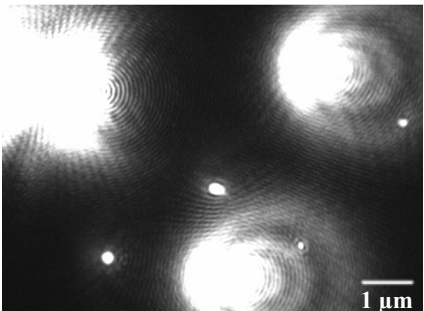
Expected pH	Nanobubbles		Nanoplastics in DI water	
	pH before $\pm$ SE	pH after $\pm$ SE	pH before $\pm$ SE	pH after $\pm$ SE
9.0	$9.14 \pm 0.15$	$7.32 \pm 0.27$	$9.10 \pm 0.04$	$7.38 \pm 0.07$
Pristine pH	$6.33 \pm 0.18$	$6.27 \pm 0.15$	$6.28 \pm 0.22$	$6.11 \pm 0.33$
5.0	$4.70 \pm 0.14$	$4.56 \pm 0.19$	$5.04 \pm 0.17$	$5.02 \pm 0.13$
3.0	$3.11 \pm 0.01$	$3.09 \pm 0.01$	$3.08 \pm 0.01$	$3.05 \pm 0.02$

**Table S2** Parameters of nanobubbles and nanoplastics used in zeta potential measurement

Sample	Material	Refractive index	Absorption
Nanobubbles	Air	1.00	0.00
Nanoplastics	Polystyrene latex	1.59	0.01



**Fig. S2.** Visible appearance of a thin film after stirring NPs with nanobubbles at pH 3.

	Before stirring	After stirring
Nanobubbles	 <p>NTA micrograph showing numerous small, bright, circular nanobubbles. A scale bar in the bottom right corner indicates 1 μm.</p>	 <p>NTA micrograph showing a few larger, bright, circular nanobubbles. A scale bar in the bottom right corner indicates 1 μm.</p>
Nanoplastics	 <p>NTA micrograph showing numerous small, bright, circular nanoplastics. A scale bar in the bottom right corner indicates 1 μm.</p>	 <p>NTA micrograph showing a few larger, bright, circular nanoplastics. A scale bar in the bottom right corner indicates 1 μm.</p>
Nanoplastics + Nanobubbles	 <p>NTA micrograph showing a mixture of small, bright, circular nanoplastics and nanobubbles. A scale bar in the bottom right corner indicates 1 μm.</p>	 <p>NTA micrograph showing a mixture of larger, bright, circular nanoplastics and nanobubbles. A scale bar in the bottom right corner indicates 1 μm.</p>

**Fig. S3.** NTA micrograph of nano-entities in the bulk phase before and after stirring at pH 3 for 5 min and 400 RPM.

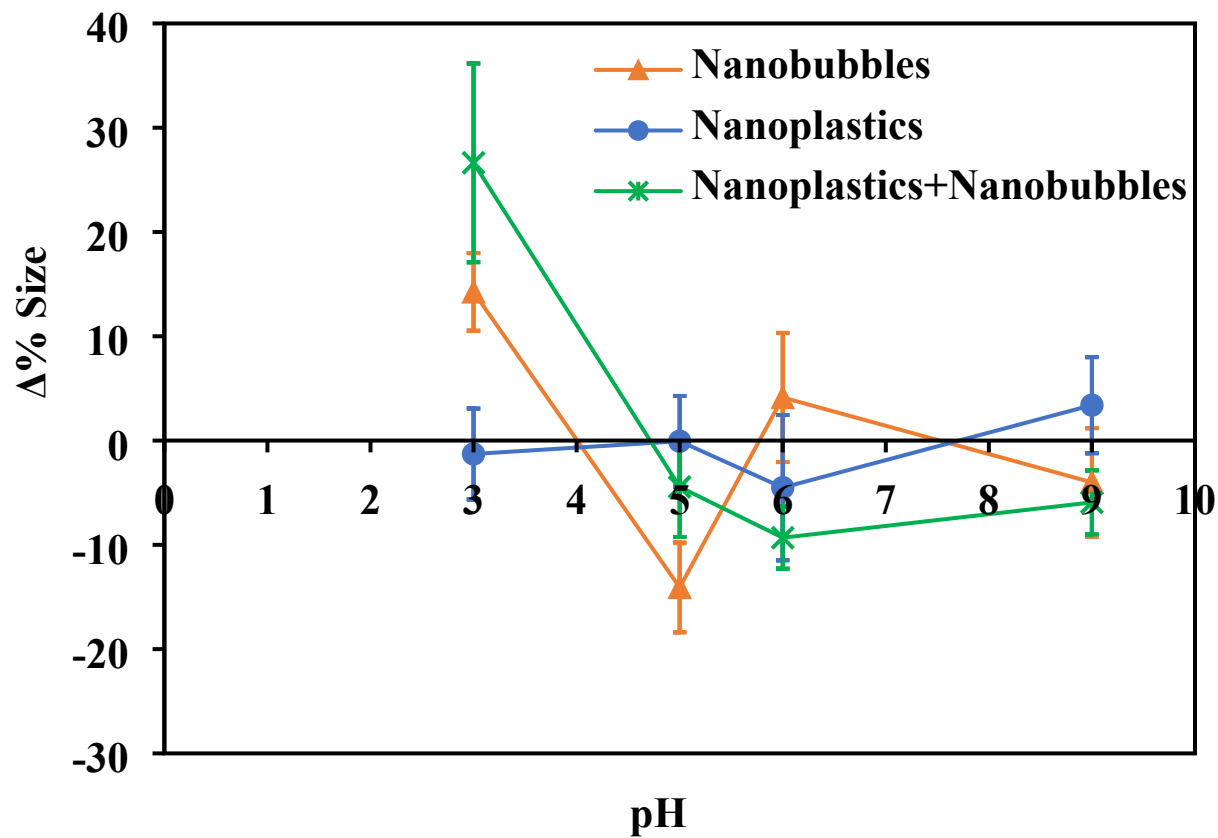


**Fig. S4.** Changes in particle size of nanobubbles, nanoplastics, and nanoplastics with nanobubbles after 5 min stirring at various pH (Conditions: initial nanoplastic concentration = 38  $\mu\text{g/L}$ , stirring speed = 400 rpm, stirring time = 5 min).



## Text S3 Rising and settling calculations

### Computations for settling velocity of nanoplastics

The following set of equations from a previous study was used to estimate the settling velocity of nanoplastics.<sup>38,39</sup> Polystyrene latex are nanospheres, hence shape factor = 1, and diameter of the nanoplastic (d) = equivalent sphere diameter

The settling velocity was calculated using Stoke's law in Eq. 1 assuming a laminar flow:

$$v_s = \frac{(\rho_p - \rho_w)d_p^2 g}{18\mu} \quad (1)$$

Where,  $v_s$  = settling velocity at laminar flow (m/s)

$\rho_p$  = density of nanoplastic (kg/m<sup>3</sup>)

$\rho_w$  = density of water at 20 °C (998.2 kg/m<sup>3</sup>)

$d_p$  = diameter of nanoplastic (m)

$g$  = acceleration due to gravity (9.81 m/s<sup>2</sup>)

$\mu$  = dynamic viscosity of water at 20 °C ( $1.002 \times 10^{-3}$  kg/m.s).

The validity of the  $v_s$  was verified by confirming with the Reynolds number (Re) (Eq. 2) given by:

$$Re = \frac{w d_p \rho_w}{\nu} \quad (2)$$

Where,  $\nu$  = kinematic viscosity of water at 20 °C ( $1.003 \times 10^{-6}$  m<sup>2</sup>/s)

$w$  = iterative settling velocity (m/s) (Eq. 3),  $w = v_s$  in the first iteration

$$w = \sqrt{\frac{4d_p}{3C_D} \left| \frac{\rho_p - \rho_w}{\rho_w} \right| g} \quad (3)$$

where,  $C_D$  = Drag coefficient (Eq. 4)

$$C_D = \frac{24}{Re}, \text{ for } Re < 0.5 \quad (4)$$

### Plastic-bubble aggregate rising velocity calculations

For flotation to occur, nanobubbles need to overcome Brownian motion and rise.<sup>40</sup> The critical size required by bubbles ( $d_b$ ) to overcome Brownian motion and rise can be calculated using Eq. 5.

$$d_b = \left( \frac{216kT\mu}{\pi g^2 (\rho_w - \rho_b)^2 t} \right)^{1/5} \quad (5)$$

Where,  $k$  = Boltzmann's constant ( $1.38 \times 10^{-23}$  J/K)

$T$  = absolute temperature (293 K)

$t$  = time (s)

$d_b$  = bubble diameter, m

According to Crittenden et al. (2012), the following expressions can be used to determine the theoretical rising velocity of a particle-bubble floc.<sup>40</sup>

The formula for calculating the density of the plastic-bubble floc ( $\rho_{pb}$ , kg/m<sup>3</sup>) is given by (Eq. 6):

$$\rho_{pb} = \frac{\rho_p d_p^3 + N_b \rho_b d_b^3}{d_p^3 + N_b d_b^3} \quad (6)$$

Where,  $\rho_b$  = air bubble density (kg/m<sup>3</sup>)

$N_b$  = number of bubbles attached to floc particle

The equivalent spherical diameter of the plastic-bubble aggregate ( $d_{pd}$ ) was determined using Eq. 7.

$$d_{pd} = (d_p^3 + N_b d_b^3)^{\frac{1}{3}} \quad (7)$$

The rising velocity of a plastic-bubble aggregate ( $v_{pb}$ ) is given by (Eq. 8):

$$v_{pb} = \left( \frac{g(\rho_w - \rho_{pb})d_{pb}^{1.75}}{33.75\rho_w^{0.25}\mu^{0.75}} \right)^{1/1.25} \quad (8)$$

The minimum volume of gas for flotation to occur is expressed by (Eq. 9):

$$\frac{\phi_g}{\phi_p} = \frac{\rho_p - \rho_w}{\rho_w - \rho_b} \quad (9)$$

Where,  $\phi_g$  = minimum volume of gas needed for flotation (mL/L)

$\phi_p$  = volume of particles (mL/L)

### Text S4 Stirring speed and velocity gradient formulas

The overall plastic-bubble collision rate depends on the rates of macroscale flocculation, microscale flocculation and differential settling flocculation between nanoplastics and nanobubbles.<sup>40</sup> Furthermore, the rate of plastic-bubble attachments ( $r_{pb}$ ) can be determined by the particle concentrations and a collision frequency function ( $\beta_{pb}$ ) as depicted in Eq. 10.

$$r_{pb} = \alpha\beta_{pb}n_p n_b \quad (10)$$

Where,  $r_{pb}$  = rate of attachment between nanoplastics and nanobubbles

$\alpha$  = collision efficiency factor (attachments per collision).  $\alpha = 1$ , assuming effective destabilization of nanoplastics and nanobubbles at pH 3.

$\beta_{pb}$  = overall collision frequency between nanoplastics and nanobubbles ( $\text{m}^3/\text{s}$ ) (Eq. 11)

$n_p$  = nanoplastics concentration

$n_b$  = nanobubbles concentration

$$\beta_{pb} = \beta_M + \beta_\mu + \beta_{DS} \quad (11)$$

$$\beta_M = \text{macroscale collision frequency, } = \frac{1}{6}G(d_p + d_b)^3 \quad (12)$$

$$\beta_\mu = \text{microscale collision frequency, } = \left(\frac{2kt}{3\mu}\right)\left(\frac{1}{d_p} + \frac{1}{d_b}\right)(d_p + d_b) \quad (13)$$

$$\beta_{DS} = \text{differential settling collision frequency, } = \frac{\pi(\rho_p - \rho_w)g}{72\mu}[(d_p + d_b)^3(d_p - d_b)] \quad (14)$$

where,  $G$  = RMS velocity gradient ( $\text{s}^{-1}$ ) (Eq. 15)

$$G = \sqrt{\frac{P}{\mu V}} \quad (15)$$

Where,  $P$  = power input of horizontal mixing ( $\text{W} = \text{kg}\cdot\text{m}^2/\text{s}^3$ ) (Eq. 16)

$V$  = volume of nanoplastic-nanobubble suspension,  $\text{m}^3$

$$P = \frac{C_{DP}A_p\rho v_R^3}{2} \quad (16)$$

Where,  $C_{DP}$  = drag coefficient on paddle (Eq. 17)

$A_p$  = projected area of paddle (m<sup>2</sup>) (Eq. 19)

$\rho$  = density of suspension = density of water (kg/m<sup>3</sup>)

$v_R$  = velocity of paddle relative to fluid (m/s) (Eq. 20)

$$C_{DP} = \frac{24}{Re} + \frac{4}{\sqrt{Re}} + 0.4 \quad (17)$$

Where,  $Re$  = Reynolds number (Eq. 18)

$$Re = \frac{D^2 N \rho}{\mu} \quad (18)$$

Where,  $D$  = diameter of impeller (0.009 m)

$N$  = impeller's rotational speed (revolutions per second)

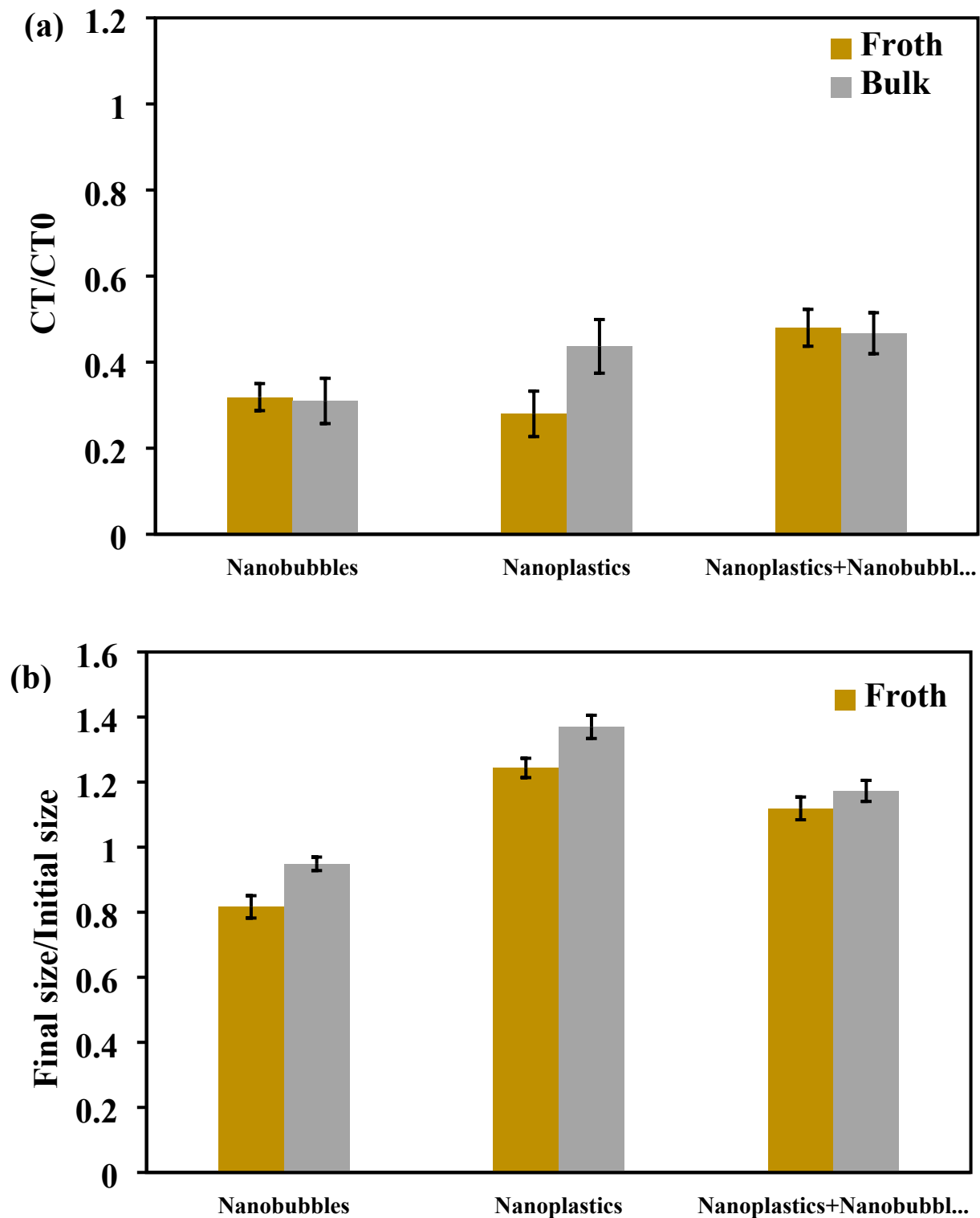
$$A_p = L \times W \quad (19)$$

Where,  $L$  = length of paddle

$W$  = width of paddle

$$v_R = 2\pi(L/2)N \times 0.75 \quad (20)$$

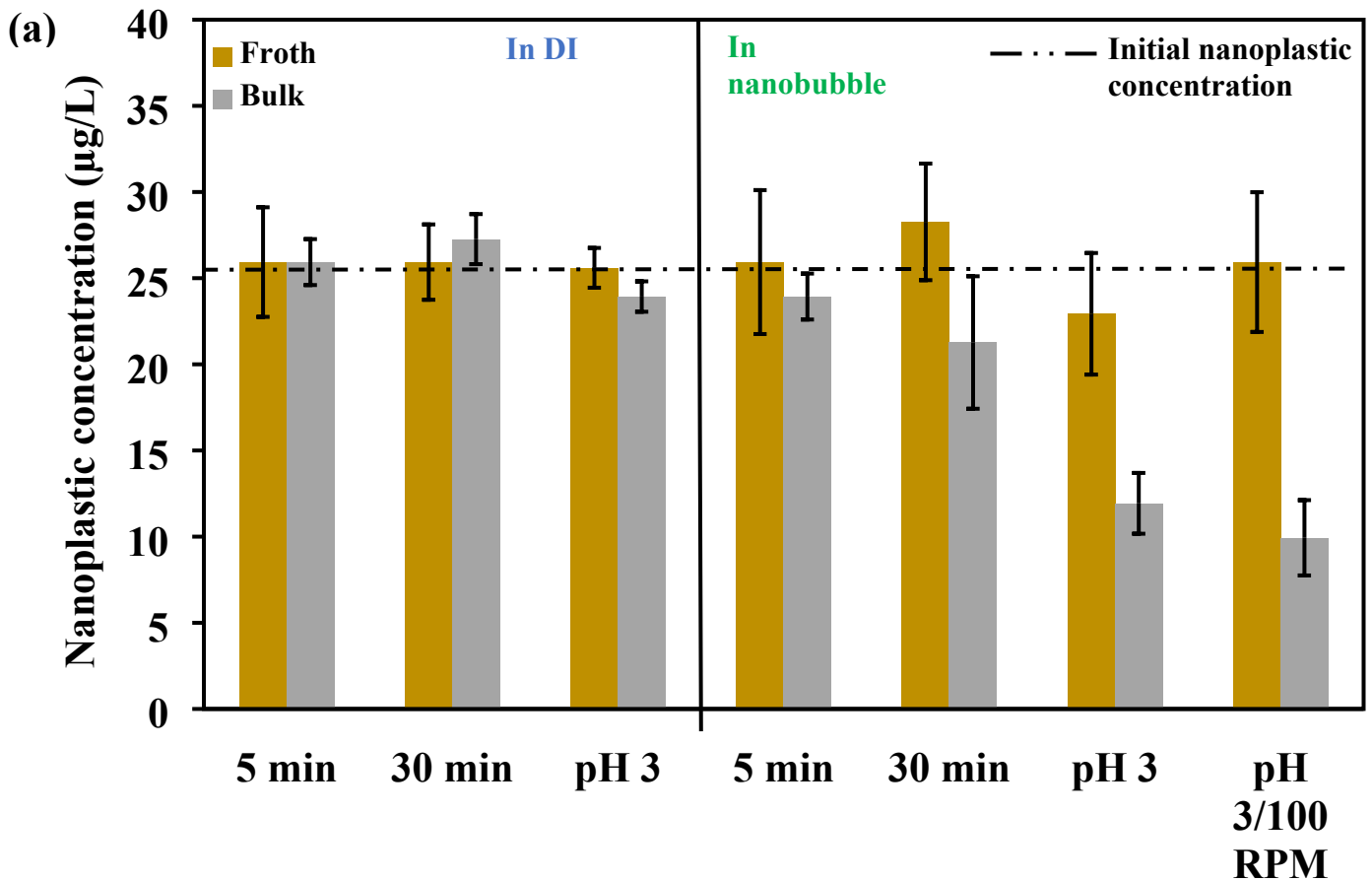
0.75 = relative velocity of paddle with respect to fluid



**Fig. S5.** (a) Normalized number concentration from NTA, and (b) Normalized average particle size distributed at the meniscus and bulk phase of DI water and nanobubble solution under static conditions (pH = 3, stirring speed = 0 RPM, 5 min).

### Text S5. Findings from the effect of stirring velocity

The velocity gradients at 400 and 100 rpm are 271 and 39 s<sup>-1</sup> respectively. Thus, the collision frequency between NPs and nanobubbles at 400 and 100 rpm was 2.8×10<sup>-11</sup> cm<sup>3</sup> s<sup>-1</sup> and 2.0×10<sup>-11</sup> cm<sup>3</sup> s<sup>-1</sup> respectively. The rate of attachment was computed as 4.2×10<sup>4</sup> cm<sup>-3</sup> s<sup>-1</sup> and 3.0×10<sup>4</sup> cm<sup>-3</sup> s<sup>-1</sup> respectively, assuming 100% attachment. A 69% of the NPs were removed at 100 rpm compared to 60% at 400 rpm based on mass concentration in the supernatant. The floc size in the float and supernatant at 100 rpm was also 28% and 13% larger respectively than that of 400 rpm. This slight increase in float mass concentration (Fig. S6a) and number concentration (Fig. S6b) at 100 rpm stirring suggests that the increased agitation and vortex formation may be re-introducing some NPs into the water column at 400 rpm. Moreover, the larger floc size at 100 rpm compared to 400 rpm implies better NP-nanobubble attachment at 100 rpm.



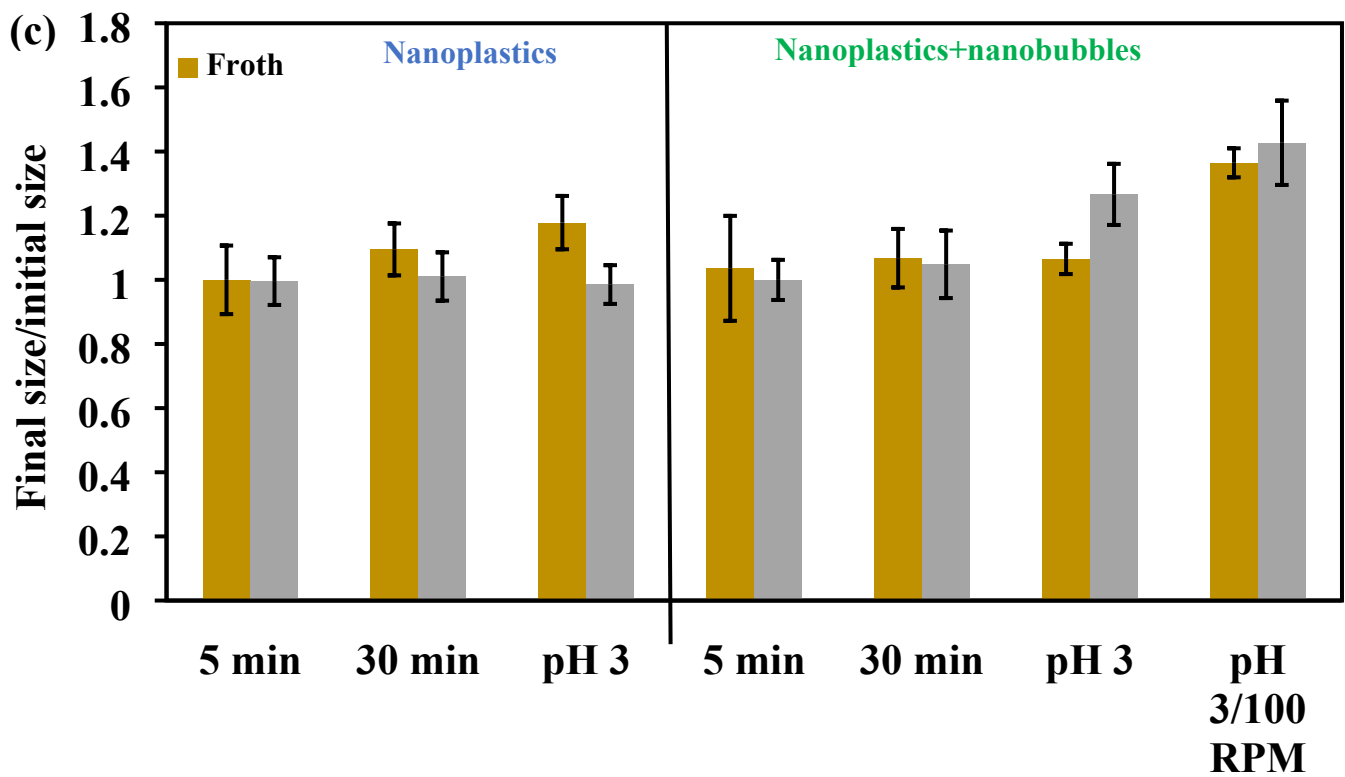
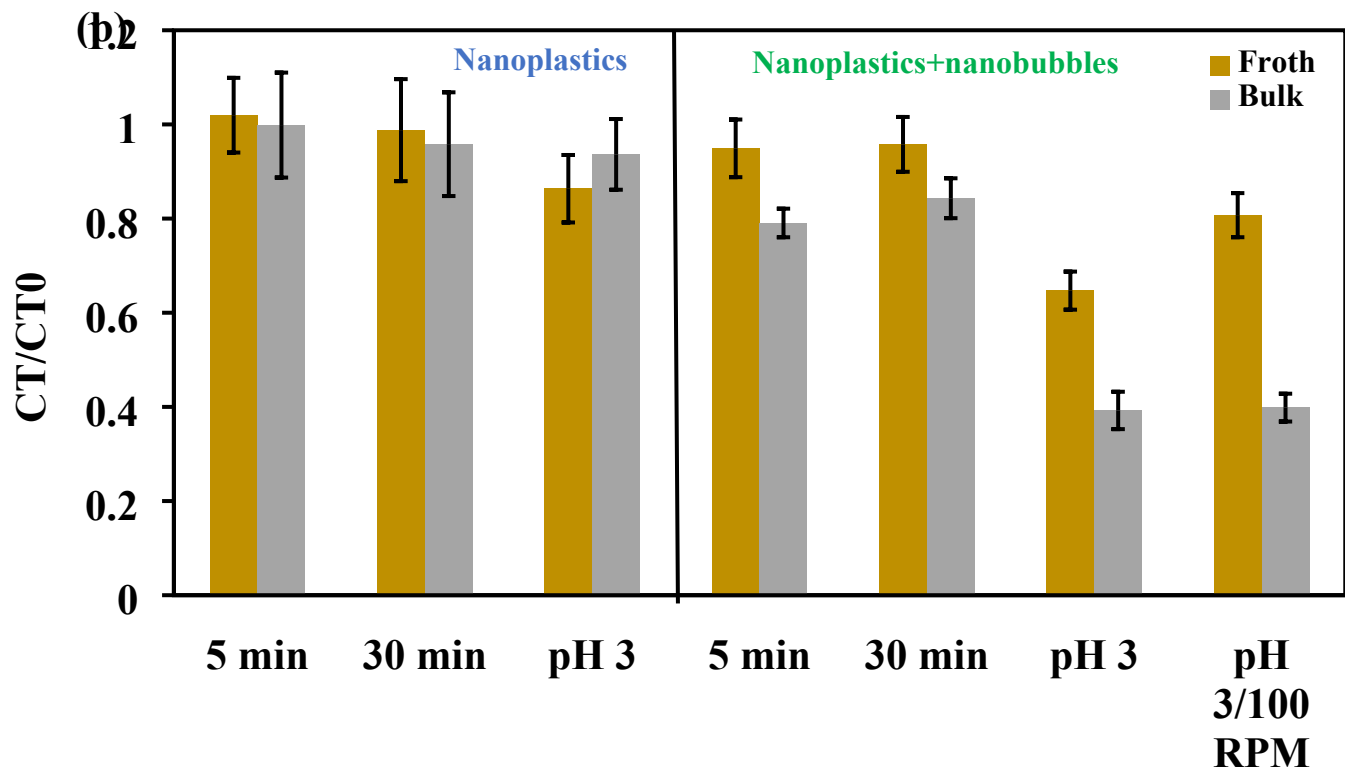




**Fig. S6.** (a) Mass concentration from UV-vis spectroscopy, (b) normalized number concentration from NTA, and (c) normalized average size of nanoplastics from NTA distributed at the meniscus and bulk phase of DI water and nanobubble solution after stirring (stirring time = 5 min unless stated otherwise, stirring speed = 400 rpm unless stated otherwise, pH is unmodified unless stated otherwise).

## References

- (1) Yang, S.; Li, M.; Kong, R. Y. C.; Li, L.; Li, R.; Chen, J.; Lai, K. P. Reproductive Toxicity of Micro- and Nanoplastics. *Environ Int* **2023**, *177*, 108002.  
<https://doi.org/10.1016/J.ENVINT.2023.108002>.
- (2) Roshanzadeh, A.; Park, S.; Ganjbakhsh, S. E.; Park, J.; Lee, D. H.; Lee, S.; Kim, E. S. Surface Charge-Dependent Cytotoxicity of Plastic Nanoparticles in Alveolar Cells under Cyclic Stretches. *Nano Lett* **2020**, *20* (10), 7168–7176.  
[https://doi.org/10.1021/ACS.NANOLETT.0C02463/SUPPL\\_FILE/NL0C02463\\_SI\\_002.MP4](https://doi.org/10.1021/ACS.NANOLETT.0C02463/SUPPL_FILE/NL0C02463_SI_002.MP4).
- (3) Liu, X.; Zhao, Y.; Dou, J.; Hou, Q.; Cheng, J.; Jiang, X. Bioeffects of Inhaled Nanoplastics on Neurons and Alteration of Animal Behaviors through Deposition in the Brain. *Nano Lett* **2022**, *22* (3), 1091–1099.  
[https://doi.org/10.1021/ACS.NANOLETT.1C04184/SUPPL\\_FILE/NL1C04184\\_SI\\_001.PDF](https://doi.org/10.1021/ACS.NANOLETT.1C04184/SUPPL_FILE/NL1C04184_SI_001.PDF).
- (4) Wan, S.; Wang, X.; Chen, W.; Xu, Z.; Zhao, J.; Huang, W.; Wang, M.; Zhang, H. Polystyrene Nanoplastics Activate Autophagy and Suppress Trophoblast Cell Migration/Invasion and Migrasome Formation to Induce Miscarriage. *ACS Nano* **2024**, *18* (4), 3733–3751. <https://doi.org/10.1021/ACSNANO.3C11734>.
- (5) Wang, J.; Qiu, W.; Cheng, H.; Chen, T.; Tang, Y.; Magnuson, J. T.; Xu, X.; Xu, E. G.; Zheng, C. Caught in Fish Gut: Uptake and Inflammatory Effects of Nanoplastics through Different Routes in the Aquatic Environment. *ACS ES&T Water* **2023**.  
<https://doi.org/10.1021/acsestwater.3c00392>.

- (6) Song, X.; Du, L.; Sima, L.; Zou, D.; Qiu, X. Effects of Micro(Nano)Plastics on the Reproductive System: A Review. *Chemosphere* **2023**, *336*, 139138.  
<https://doi.org/10.1016/J.CHEMOSPHERE.2023.139138>.
- (7) He, Y.; Li, J.; Chen, J.; Miao, X.; Li, G.; He, Q.; Xu, H.; Li, H.; Wei, Y. Cytotoxic Effects of Polystyrene Nanoplastics with Different Surface Functionalization on Human HepG2 Cells. *Science of The Total Environment* **2020**, *723*, 138180.  
<https://doi.org/10.1016/J.SCITOTENV.2020.138180>.
- (8) Alimi, O. S.; Farner Budarz, J.; Hernandez, L. M.; Tufenkji, N. Microplastics and Nanoplastics in Aquatic Environments: Aggregation, Deposition, and Enhanced Contaminant Transport. *Environ Sci Technol* **2018**, *52* (4), 1704–1724.  
[https://doi.org/10.1021/ACS.EST.7B05559/SUPPL\\_FILE/ES7B05559\\_SI\\_001.PDF](https://doi.org/10.1021/ACS.EST.7B05559/SUPPL_FILE/ES7B05559_SI_001.PDF).
- (9) Sun, X.; Chen, B.; Li, Q.; Liu, N.; Xia, B.; Zhu, L.; Qu, K. Toxicities of Polystyrene Nano- and Microplastics toward Marine Bacterium *Halomonas Alkaliphila*. *Science of The Total Environment* **2018**, *642*, 1378–1385.  
<https://doi.org/10.1016/J.SCITOTENV.2018.06.141>.
- (10) Chen, Q.; Reisser, J.; Cunsolo, S.; Kwadijk, C.; Kotterman, M.; Proietti, M.; Slat, B.; Ferrari, F. F.; Schwarz, A.; Levivier, A.; Yin, D.; Hollert, H.; Koelmans, A. A. Pollutants in Plastics within the North Pacific Subtropical Gyre. *Environ Sci Technol* **2018**, *52* (2), 446–456. [https://doi.org/10.1021/ACS.EST.7B04682/ASSET/IMAGES/LARGE/ES-2017-04682T\\_0003.JPEG](https://doi.org/10.1021/ACS.EST.7B04682/ASSET/IMAGES/LARGE/ES-2017-04682T_0003.JPEG).
- (11) Gigault, J.; Halle, A. ter; Baudrimont, M.; Pascal, P. Y.; Gauffre, F.; Phi, T. L.; El Hadri, H.; Grassl, B.; Reynaud, S. Current Opinion: What Is a Nanoplastic? *Environmental*

*Pollution*. Elsevier Ltd April 1, 2018, pp 1030–1034.

<https://doi.org/10.1016/j.envpol.2018.01.024>.

- (12) van Wijnen, J.; Ragas, A. M. J.; Kroeze, C. Modelling Global River Export of Microplastics to the Marine Environment: Sources and Future Trends. *Science of the Total Environment* **2019**, *673*, 392–401. <https://doi.org/10.1016/j.scitotenv.2019.04.078>.
- (13) Liu, Z.; Yu, P.; Cai, M.; Wu, D.; Zhang, M.; Huang, Y.; Zhao, Y. Polystyrene Nanoplastic Exposure Induces Immobilization, Reproduction, and Stress Defense in the Freshwater Cladoceran *Daphnia Pulex*. *Chemosphere* **2019**, *215*, 74–81. <https://doi.org/10.1016/J.CHEMOSPHERE.2018.09.176>.
- (14) Pedersen, A. F.; Meyer, D. N.; Petriv, A. M. V.; Soto, A. L.; Shields, J. N.; Akemann, C.; Baker, B. B.; Tsou, W. L.; Zhang, Y.; Baker, T. R. Nanoplastics Impact the Zebrafish (*Danio Rerio*) Transcriptome: Associated Developmental and Neurobehavioral Consequences. *Environmental Pollution* **2020**, *266*, 115090. <https://doi.org/10.1016/J.ENVPOL.2020.115090>.
- (15) González-Fernández, C.; Tallec, K.; Le Goïc, N.; Lambert, C.; Soudant, P.; Huvet, A.; Suquet, M.; Berchel, M.; Paul-Pont, I. Cellular Responses of Pacific Oyster (*Crassostrea Gigas*) Gametes Exposed in Vitro to Polystyrene Nanoparticles. *Chemosphere* **2018**, *208*, 764–772. <https://doi.org/10.1016/J.CHEMOSPHERE.2018.06.039>.
- (16) Xie, X.; Deng, T.; Duan, J.; Xie, J.; Yuan, J.; Chen, M. Exposure to Polystyrene Microplastics Causes Reproductive Toxicity through Oxidative Stress and Activation of the P38 MAPK Signaling Pathway. *Ecotoxicol Environ Saf* **2020**, *190*, 110133. <https://doi.org/10.1016/J.ECOENV.2019.110133>.

- (17) Duan, Z.; Duan, X.; Zhao, S.; Wang, X.; Wang, J.; Liu, Y.; Peng, Y.; Gong, Z.; Wang, L. Barrier Function of Zebrafish Embryonic Chorions against Microplastics and Nanoplastics and Its Impact on Embryo Development. *J Hazard Mater* **2020**, *395*, 122621. <https://doi.org/10.1016/J.JHAZMAT.2020.122621>.
- (18) van Wijnen, J.; Ragas, A. M. J.; Kroeze, C. Modelling Global River Export of Microplastics to the Marine Environment: Sources and Future Trends. *Science of the Total Environment* **2019**, *673*, 392–401. <https://doi.org/10.1016/j.scitotenv.2019.04.078>.
- (19) Yin, K.; Wang, Y.; Zhao, H.; Wang, D.; Guo, M.; Mu, M.; Liu, Y.; Nie, X.; Li, B.; Li, J.; Xing, M. A Comparative Review of Microplastics and Nanoplastics: Toxicity Hazards on Digestive, Reproductive and Nervous System. *Science of the Total Environment*. Elsevier B.V. June 20, 2021. <https://doi.org/10.1016/j.scitotenv.2021.145758>.
- (20) Alimi, O. S.; Farner Budarz, J.; Hernandez, L. M.; Tufenkji, N. Microplastics and Nanoplastics in Aquatic Environments: Aggregation, Deposition, and Enhanced Contaminant Transport. *Environmental Science and Technology*. American Chemical Society February 20, 2018, pp 1704–1724. <https://doi.org/10.1021/acs.est.7b05559>.
- (21) Collins, A.; Ateia, M.; Bhagat, K.; Ohno, T.; Perreault, F.; Apul, O. Emerging Investigator Series: Microplastic-Based Leachate Formation under UV Irradiation: The Extent, Characteristics, and Mechanisms. *Environ Sci (Camb)* **2022**, *9* (2), 363–374. <https://doi.org/10.1039/d2ew00423b>.
- (22) Hong, J.; Lee, B.; Park, C.; Kim, Y. Novel Measurement Method of Determining PS Nanoplastic Concentration via AuNPs Aggregation with NaCl. *Korean Journal of*

- Chemical Engineering* **2022**, 39 (10), 2842–2848. <https://doi.org/10.1007/s11814-022-1153-9>.
- (23) Swart, B.; Pihlajamäki, A.; John Chew, Y. M.; Wenk, J. Microbubble-Microplastic Interactions in Batch Air Flotation. *Chemical Engineering Journal* **2022**, 449. <https://doi.org/10.1016/j.cej.2022.137866>.
- (24) Yeo, I. C.; Shim, K. Y.; Kim, K.; Go, Y. S.; Kim, J.; Lee, D. H.; Lee, J. S.; Shin, K. H.; Jeong, C. B. Insights into Tissue-Specific Bioaccumulation of Nanoplastics in Marine Medaka as Revealed by a Stable Carbon Isotopic Approach. *Environ Sci Technol Lett* **2023**. <https://doi.org/10.1021/acs.estlett.3c00651>.
- (25) Yeo, I.-C.; Shim, K.-Y.; Kim, K.; Go, Y.-S.; Kim, J.; Lee, D.-H.; Lee, J.-S.; Shin, K.-H.; Jeong, C.-B. Insights into Tissue-Specific Bioaccumulation of Nanoplastics in Marine Medaka as Revealed by a Stable Carbon Isotopic Approach. *Environ Sci Technol Lett* **2023**, 10 (10), 838–843. <https://doi.org/10.1021/ACS.ESTLETT.3C00651>.
- (26) Estrela, F. N.; Batista Guimarães, A. T.; Silva, F. G.; Marinho da Luz, T.; Silva, A. M.; Pereira, P. S.; Malafaia, G. Effects of Polystyrene Nanoplastics on Ctenopharyngodon Idella (Grass Carp) after Individual and Combined Exposure with Zinc Oxide Nanoparticles. *J Hazard Mater* **2021**, 403. <https://doi.org/10.1016/j.jhazmat.2020.123879>.
- (27) Pérez-Reverón, R.; Álvarez-Méndez, S. J.; González-Sálamo, J.; Socas-Hernández, C.; Díaz-Peña, F. J.; Hernández-Sánchez, C.; Hernández-Borges, J. Nanoplastics in the Soil Environment: Analytical Methods, Occurrence, Fate and Ecological Implications. *Environmental Pollution* **2023**, 317, 120788. <https://doi.org/10.1016/J.ENVPOL.2022.120788>.

- (28) Rout, P. R.; Mohanty, A.; Aastha; Sharma, A.; Miglani, M.; Liu, D.; Varjani, S. Micro- and Nanoplastics Removal Mechanisms in Wastewater Treatment Plants: A Review. *Journal of Hazardous Materials Advances* **2022**, *6*.  
<https://doi.org/10.1016/j.hazadv.2022.100070>.
- (29) Onyedibe, V.; Kakar, F. L.; Okoye, F.; Elbeshbishy, E.; Hamza, R. Sources and Occurrence of Microplastics and Nanoplastics in the Environment. In *Current Developments in Biotechnology and Bioengineering: Microplastics and Nanoplastics: Occurrence, Environmental Impacts and Treatment Processes*; Elsevier, 2022; pp 33–58.  
<https://doi.org/10.1016/B978-0-323-99908-3.00019-1>.
- (30) Lai, H.; Liu, X.; Qu, M. Nanoplastics and Human Health: Hazard Identification and Biointerface. *Nanomaterials*. MDPI April 1, 2022. <https://doi.org/10.3390/nano12081298>.
- (31) Joksimovic, N.; Selakovic, D.; Jovicic, N.; Jankovic, N.; Pradeepkumar, P.; Eftekhari, A.; Rosic, G. Nanoplastics as an Invisible Threat to Humans and the Environment. *Journal of Nanomaterials*. Hindawi Limited 2022. <https://doi.org/10.1155/2022/6707819>.
- (32) Chen, Y.; Xu, H.; Luo, Y.; Ding, Y.; Huang, J.; Wu, H.; Han, J.; Du, L.; Kang, A.; Jia, M.; Xiong, W.; Yang, Z. Plastic Bottles for Chilled Carbonated Beverages as a Source of Microplastics and Nanoplastics. *Water Res* **2023**, *242*.  
<https://doi.org/10.1016/j.watres.2023.120243>.
- (33) Huang, D.; Tao, J.; Cheng, M.; Deng, R.; Chen, S.; Yin, L.; Li, R. Microplastics and Nanoplastics in the Environment: Macroscopic Transport and Effects on Creatures. *Journal of Hazardous Materials*. Elsevier B.V. April 5, 2021.  
<https://doi.org/10.1016/j.jhazmat.2020.124399>.

- (34) Davranche, M.; Lory, C.; Juge, C. Le; Blancho, F.; Dia, A.; Grassl, B.; El Hadri, H.; Pascal, P. Y.; Gigault, J. Nanoplastics on the Coast Exposed to the North Atlantic Gyre: Evidence and Traceability. *NanoImpact* **2020**, *20*.  
<https://doi.org/10.1016/j.impact.2020.100262>.
- (35) Xiao, F.; Feng, L. J.; Sun, X. D.; Wang, Y.; Wang, Z. W.; Zhu, F. P.; Yuan, X. Z. Do Polystyrene Nanoplastics Have Similar Effects on Duckweed (*Lemna Minor* L.) at Environmentally Relevant and Observed-Effect Concentrations? *Environ Sci Technol* **2022**, *56* (7), 4071–4079. <https://doi.org/10.1021/acs.est.1c06595>.
- (36) Kanematsu, W.; Tuziuti, T.; Yasui, K. The Influence of Storage Conditions and Container Materials on the Long Term Stability of Bulk Nanobubbles — Consideration from a Perspective of Interactions between Bubbles and Surroundings. *Chem Eng Sci* **2020**, *219*, 115594. <https://doi.org/10.1016/j.ces.2020.115594>.
- (37) Yaparathne, S.; Doherty, Z. E.; Magdaleno, A. L.; Matula, E. E.; MacRae, J. D.; Garcia-Segura, S.; Apul, O. G. Effect of Air Nanobubbles on Oxygen Transfer, Oxygen Uptake, and Diversity of Aerobic Microbial Consortium in Activated Sludge Reactors. *Bioresour Technol* **2022**, *351*. <https://doi.org/10.1016/j.biortech.2022.127090>.
- (38) Waldschläger, K.; Born, M.; Cowger, W.; Gray, A.; Schüttrumpf, H. Settling and Rising Velocities of Environmentally Weathered Micro- and Macroplastic Particles. *Environ Res* **2020**, *191*. <https://doi.org/10.1016/j.envres.2020.110192>.
- (39) Metcalf & Eddy; Abu-Orf, M.; Bowden, G.; Burton, F. L.; Pfrang, W.; Stensel, H. D.; Tchobanoglous, G.; Tsuchihashi, R.; AECOM (Firm). *Wastewater Engineering: Treatment and Resource Recovery*, 5th ed.; McGraw Hill Education: New York, 2014.



- (40) Crittenden, J. C. (John C.; Montgomery Watson Harza (Firm)). *MWH's Water Treatment : Principles and Design*, 3rd ed.; John Wiley & Sons, 2012.